Cancer Letters 449 (2019) 76–86

Contents lists available at ScienceDirect

Cancer Letters

journal homepage: www.elsevier.com/locate/canlet

Original Articles

TOX3 inhibits cancer cell migration and invasion via transcriptional regulation of SNAI1 and SNAI2 in clear cell renal cell carcinoma

Bo Jiang[a,1], Wei Chen[a,1], Haixiang Qin[a,1], Wenli Diao[a], Binghua Li[b], Wenmin Cao[a], Zhenxing Zhang[c], Wei Qi[c], Jie Gao[a], Mengxia Chen[a], Xiaozhi Zhao[a,**], Hongqian Guo[a,*]

[a] Department of Urology, Drum Tower Hospital, Medical School of Nanjing University, Institute of Urology, Nanjing University, 321 Zhongshan Road, Nanjing, 210008, Jiangsu, PR China
[b] Department of Hepatobiliary Surgery, Drum Tower Hospital, Medical School of Nanjing University, Nanjing, 210008, Jiangsu, PR China
[c] Department of Urology, Drum Tower Hospital, Clinical College of Nanjing Medical University, Nanjing, 210008, Jiangsu, PR China

ARTICLE INFO

Keywords:
TOX3
Clear cell renal cell carcinoma (ccRCC)
Migration
Invasion
Transcriptional regulation

ABSTRACT

Studies on the mechanism of clear cell renal cell carcinoma (ccRCC) progression are lacking. In this study, TOX3 was identified as a novel cancer suppressor gene in ccRCC. Hypermethylation of CpG probes in the promoter region was associated with the functional loss of TOX3 in ccRCC cancer tissues. Downregulation of TOX3 mRNA was strongly associated with poor clinical outcomes in ccRCC. Immunohistochemistry confirmed TOX3 was downregulated in primary tumors without metastasis (n = 126) and further downregulated in primary metastatic tumors (n = 23) compared with adjacent noncancerous tissues (n = 92). In vitro, overexpression of TOX3 inhibited RCC cell growth, migration and invasion. Mechanistic investigations showed that TOX3 deficiency facilitates the epithelial-mesenchymal transition due to impairment of transcriptional repression of SNAIL members SNAI1 and SNAI2 and promotes cancer cell migration and invasion. In vivo, restoring TOX3 expression reduced lung metastatic lesions and prolonged survival of mice. TOX3 combined with SNAI1 or SNAI2 predicted overall survival in ccRCC patients. Blockage of this pathway could be a promising therapeutic target for advanced ccRCC.

1. Introduction

Renal cell carcinoma (RCC) represents 3%–4% of adult malignancies with clear cell the most common pathological type [1]. Metastases often occur in advanced stages of cancer and imply poor prognosis; the 5 year survival rate of metastatic RCC (mRCC) is less than 10% because of resistance to chemotherapy and radiotherapy [2]. Tyrosine kinase inhibitors, have been widely used to control mRCC progression [3,4]; however, they were associated with limited survival benefit and severe side effects [5]. Poor clinical outcomes and limitations of treatment urgently require further mechanistic studies of tumor progression for more efficient anti-tumor treatments. In this study, we used a screening program and identified TOX high mobility group box family member 3 (TOX3) as a novel cancer suppressor gene of ccRCC.

TOX3 (also known as TNRC9 and CAGF9) is a conserved protein and belongs to the HMG-box protein family [6]. HMG-box family proteins can distort DNA and affect their transcription, potentially allowing simultaneous binding of other transcriptional regulators to DNA [7,8]. TOX3 has been reported to interact with CBP/CREB or CBP/CITED1 complex [9,10], and protect the nervous system against spinal cord injury [11]. In addition, single nucleotide polymorphisms (SNPs) of TOX3 were found closely associated with breast cancer and lung cancer risk [12,13], however, the role of TOX3 in renal cancer progression and metastasis have not been revealed.

Metastatic dissemination is often initiated by reprogramming of cells associated with the epithelial-mesenchymal transition (EMT) [14,15]. To achieve mobility and invasiveness, cancer cells are considered to use loss of apical-basal polarity and cell-cell junctions and gain of a mesenchymal phenotype [16,17]. Functional loss of E-cadherin, a hallmark of EMT, is associated with metastatic progression in human RCC [18]. In addition, expression of SNAIL family members, such as the EMT-inducing transcription factors SNAI1/Snail1 and SNAI2/Slug, contribute to the invasion ability of cells in renal cancer [19,20] and other malignancies [21–23].

* Corresponding author.
** Corresponding author.
E-mail addresses: zhaoxz@nju.edu.cn (X. Zhao), dr.ghq@nju.edu.cn (H. Guo).
[1] These authors contributed equally to this work.

https://doi.org/10.1016/j.canlet.2019.02.020
Received 25 October 2018; Received in revised form 7 February 2019; Accepted 10 February 2019

In this study, we found that TOX3 significantly downregulated in ccRCC tissue and associated with cell invasive activity in ccRCC. Loss of TOX3 was verified to be correlated with advanced clinical stage and adverse prognosis of ccRCC. Downregulation of TOX3 could accelerate the EMT by decreasing transcriptional repression of SNAI1 and SNAI2. These data support a novel cancer suppressor role of TOX3 and provide new insights into the progression of ccRCC.

2. Materials and methods

2.1. Patients and clinical samples

Frozen ccRCC tissues and noncancerous kidney tissues for quantitative real-time PCR (n = 22) and western blot (n = 8) as well as formalin-fixated ccRCC tissues (n = 151) and noncancerous kidney tissues (n = 92) for immunohistochemistry were collected from patients undergoing surgical resection from 2008 to 2017. Cancerous tissues was classified as the clear cell type according to the WHO classification at the Medical School of Nanjing University affiliated Nanjing Drum Tower Hospital. Microvascular invasion was defined as tumor thrombus or invasion of tumor cells in microscopic vessels (excluding renal vein and its segmental branches and inferior vena cava) [24]. Patients' clinical and pathological information were collected and written informed consent was obtained from each patient.

2.2. Bioinformatics analysis

Array data for GSE14994, GSE15641, GSE11151, GSE6344, GSE781 were obtained from the Oncomine database (https://www.oncomine.org/). Processed TCGA (The Cancer Genome Atlas) Level 3 RNA-seq data (Illumina HiseqV2), DNA methylation microarray data (Illumina Infinium Human Methylation450 BeadChip) and Level 1 clinical data (version: 2016-01-28) were obtained from the Broad Institute Genome Data Analysis Center (GDAC) Firehose, gene normalized abundance estimates were calculated with the RSEM method and then RNA-Seq normalized counts were log-transformed. Gene Set Enrichment Analysis (GSEA) was used to analyze TCGA data according to the manufacturer's protocol.

2.3. Cell lines and cell culture

Human RCC cell line (A498) was purchased from National Infrastructure of Cell Line Resource (Beijing) and 769-P, 786-O, Caki-1 and ACHN cell lines were obtained from the Cell Bank of the Chinese Academy of Science (Shanghai). Murine RCC cell line (Renca) was purchased from the American Type Culture Collection (Rockville, MD, USA). 769-P, 786-O and Renca cells were cultured in RPMI 1640 medium with 10% fetal bovine serum (FBS) (Gibco). Caki-1 and ACHN cells were cultured in McCoy' 5A medium and DMEM medium with 10% FBS, respectively. All complete medium was supplemented with 100 U/mL penicillin and 100 μg/mL streptomycin.

2.4. Quantitative real-time PCR (qRT-PCR)

Total RNA was extracted with TRIzol reagent (Invitrogen Biotech). cDNA synthesis of genes involved using PrimeScript RT Master Mix (TaKaRa Biotech). qRT-PCR involved use of SYBR Premix Ex Taq (TaKaRa Biotech) with the StepOne Real-Time PCR System. Relative mRNA expression was normalized to that of ACTB by the $2^{-\triangle\triangle CT}$ method. The primer sequences are in Supplementary Table S2.

2.5. Immunohistochemistry (IHC)

Clinical ccRCC and noncancerous specimens and pulmonary metastatic samples were used for IHC. Staining intensity was scored as 0 (negative), 1 (low), 2 (moderate), and 3 (high). Staining range was scored as 0 (0% stained), 1 (1%–25% stained), 2 (26%–50% stained), 3 (51%–75% stained) and 4 (> 75% stained). The final score was obtained by multiplying the intensity scores by staining range, for the final scores (intensity score × percentage score); a score ≤4 was defined as low expression and > 4 high expression.

2.6. Transwell migration and invasion assay

For migration assay, cells were digested and resuspended in conditioned medium, 786-O cells (2×10^4 cells) and 769-P cells (5×10^4 cells) were seeded in the upper transwell chamber (8 μm, Corning Inc.); the lower chamber was covered with complete medium. Transwell chambers were collected after 12 h. For invasion assay, diluted matrigel (BD Biosciences) was spread on the bottom of the upper chamber, and 786-O cells (2×10^4 cells) and 769-P cells (5×10^4 cells) were seeded in the upper chamber; chambers were collected after 12 h. Finally, cells were fixed, then stained with the Crystal Violet Staining Solution (Beyotime Biotech).

2.7. Chromatin immunoprecipitation

Chromatin immunoprecipitation (ChIP) assay of 769-P cells involved use of the SimpleChIP Plus Sonication Chromatin IP Kit (Cell Signaling Technology) with an antibody for TOX3 and anti-rabbit IgG as the negative control according to the user's manual. Lysates were immunoprecipitated with an antibody for TOX3, normal rabbit IgG, and antibody for H3 as positive control. The ChIP DNA samples were detected with specific primers listed in Supplementary Table S2.

2.8. Animal experiments

Six-week-old male BALB/c mice were purchased from the Animal Core Facility of Nanjing Medical University. Cells in each groups (2×10^6 in 0.1 mL sterilized PBS) were injected into the right axilla of mice. Subcutaneous tumors were resected after 2 weeks. Tumor volume (longest diameter × shortest diameter^2/2) and weight were measured. For pulmonary metastatic models, cells in each group (1×10^5 cells) were injected in the tail vein of mice; mice were killed after 1 month, then lungs were harvested to assess pulmonary metastasis. For analysis of survival, cells in each group (1×10^5 cells) were injected in the tail vein of mice; the survival time of mice was recorded for survival analysis. For evaluating the therapeutic effect of 5-azacytidine (5-Aza) (Sigma), one week after subcutaneous tumor incubation, mice were intraperitoneal injected with 2.5 mg/kg 5-Aza three times a week for two weeks, then tumors were resected and measured. Same treatment was immediately delivered after establishment of lung metastatic model with Renca-luci (luciferase) cells (1×10^5 cells), lungs were harvested to assess metastasis after three weeks drug intervention. Lung metastatic nodules were monitored *in vivo* with IVIS spectrum imaging system. The signal intensity of *luci*-labeled cells from lung tissues represented the amount of lung metastatic lesions. All animal studies were conducted according to the guidelines of the Institutional Animal Care and Use Committee of Nanjing Drum Tower Hospital.

2.9. Statistical analysis

IBM SPSS Statistics 21 and Graphpad prism 6 were used for analysis. Normally distributed data are expressed as mean ± SD and were compared by Student *t*-test. Categorical data were analyzed by Fisher exact test or chi-square test. Correlations analysis involved the Pearson coefficient. Kaplan-Meier and Log-rank tests were used for analysis of overall survival and metastatic-free survival. $p < 0.05$ was considered statistically significantly.

Other experimental methods please refer to the Supplementary Methods for details.

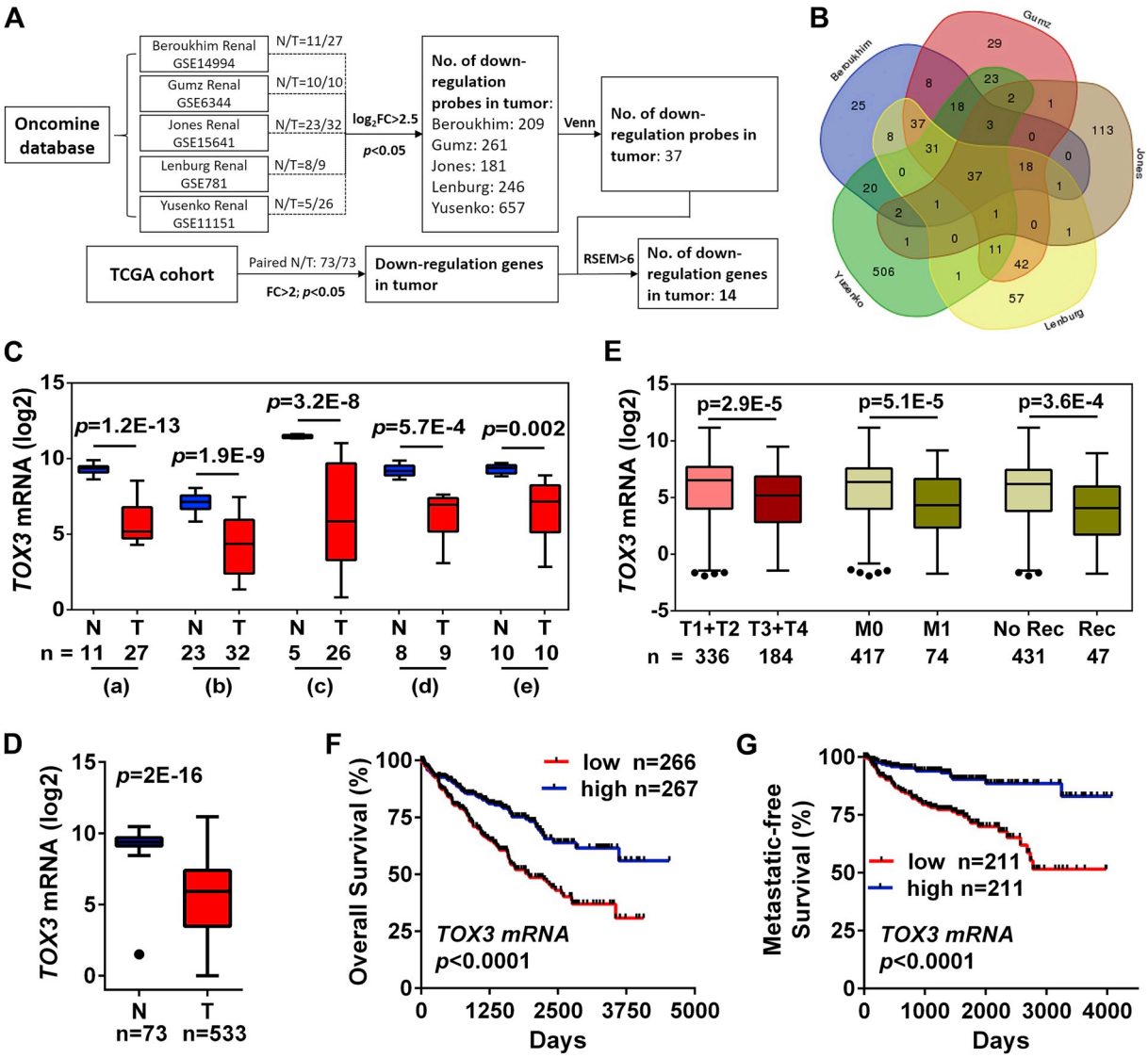

Fig. 1. Identification of TOX3 as a candidate cancer suppressor gene in ccRCC. (A) Screening program of candidate cancer suppressor genes of ccRCC in the Oncomine database and TCGA database. FC = fold change, N = noncancerous tissues, T = cancerous tissues. (B) Venn-diagram analysis of down-regulated genes in five independent GEO datasets Beroukhim Renal (GSE14994), Gumz Renal (GSE6344), Jones Renal (GSE15641), Lenburg Renal (GSE781) and Yusenko Renal (GSE11151) from the Oncomine database. (C) Boxplots with TOX3 (representative probe: 214774_x_at) mRNA levels (log2) on the y-axis and N vs T on the x-axis. Data are from GSE14994 (a), GSE15641 (b), GSE11151 (c), GSE781 (d), GSE6344 (e). (D) The mRNA level of TOX3 in ccRCC tissues (n = 534) from the TCGA database and adjacent noncancerous tissues (n = 72). (E) Clinical characteristics of TOX3 expression for ccRCC patients in the TCGA database by clinical T stage, distant metastasis or not (M0 and M1) and recurrence status (Rec). (F–G) Kaplan-Meier analysis of overall survival ($p < 0.0001$) and metastatic-free survival ($p < 0.0001$) for ccRCC patients with low or high levels of TOX3 in the TCGA database.

3. Results

3.1. Identification of TOX3 as a candidate cancer suppressor gene in ccRCC

To identify the novel suppressor genes in ccRCC, we screened genes by analyzing all GEO datasets containing Affymetrix U133A Array or U133 Plus 2.0 Array data for ccRCC cancerous and noncancerous tissues in the Oncomine database (GEO accessions: GSE14994, GSE15641, GSE11151, GSE6344, GSE781) (Fig. 1A) [25–29]. A five-way Venn diagram shows the 37 shared downregulated probes in ccRCC tissues compared with noncancerous tissues ($Log_2FC > 2.5$, $p < 0.05$) (Fig. 1B). Genes corresponding to these probes were verified in the TCGA ccRCC cohort [fold change > 2.0, $p < 0.05$, Log_2(normalized count) > 6.0]; 14 candidate ccRCC suppressor genes were identified and are listed in Supplementary Table S1. While some of them, such as *SCNN1A*, *MAL*, *ACSF2*, did not show very significant correlation ($p > 0.0001$) with overall survival (OS) compared with *TOX3*, *ALDOB* and *ALDH6A1* ($p < 0.0001$, Supplementary Fig. S1). Besides, several studies have revealed that genetic polymorphisms in TOX3 were associated with clinical outcome of breast and lung cancer (*12, 13*), so we focused our attention on the role of TOX3 in ccRCC progression. TOX3 showed significantly decreased expression in cancerous tissues (Fig. 1C–D) which was strongly associated with prognosis in ccRCC ($p < 0.0001$, Supplementary Fig. S1). TOX3 downregulated in papillary RCC (pRCC) cancerous tissues as well (Supplementary Fig. S2C). Clinical association studies of data for the TCGA cohort revealed downregulated TOX3 mRNA significantly associated with advanced T stage, distant metastasis and recurrence (Fig. 1E). TOX3 level and histological grade or lymphatic metastasis were not associated despite the downward trend of TOX3 level in higher-grade and lymph node-positive tumors (Supplementary Figs. S2A–B). Moreover, OS and metastatic-free survival (MFS) were shortened for ccRCC patients with TOX3

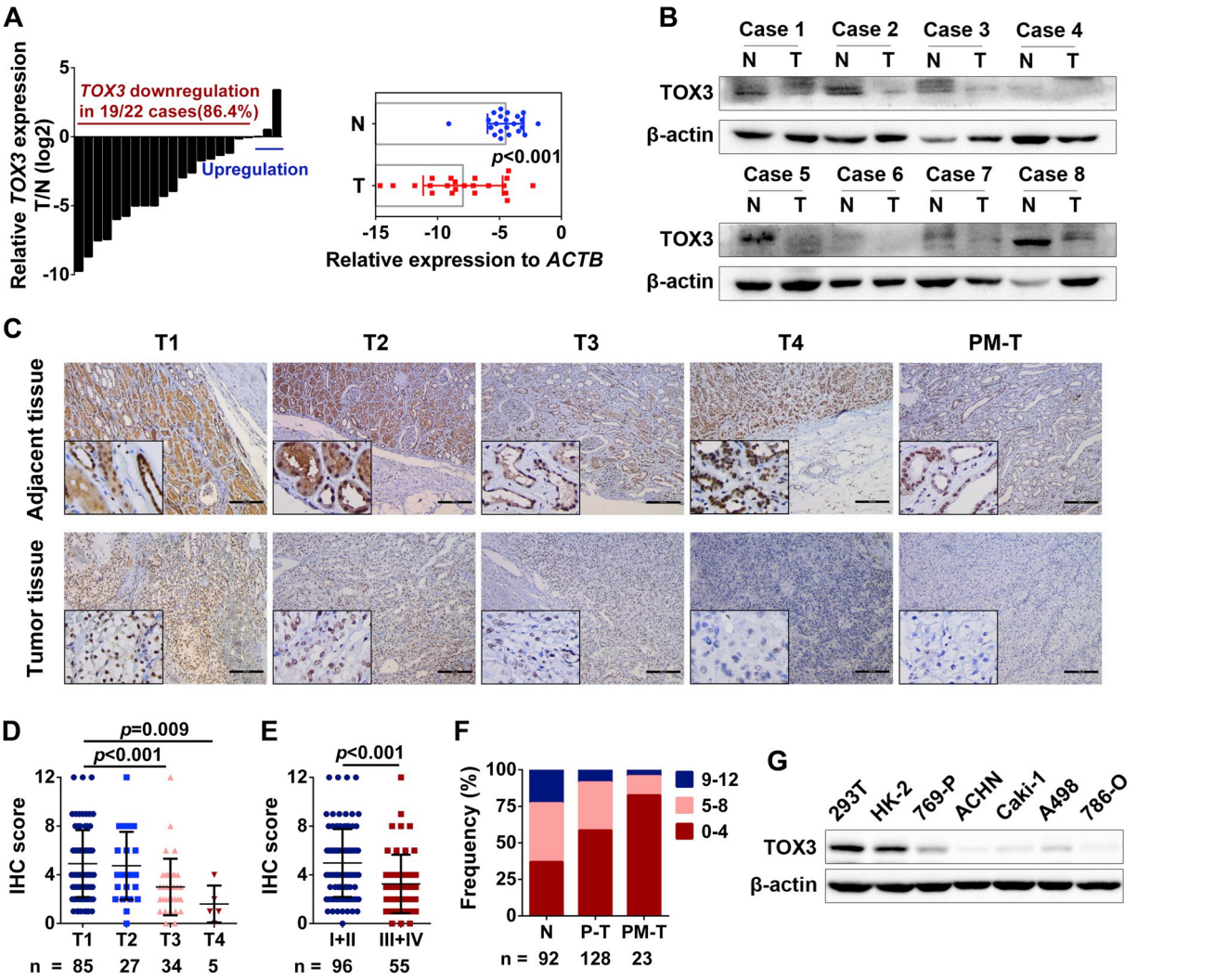

Fig. 2. Validation of TOX3 down-regulation in ccRCC clinical specimens and cell lines. (A) Quantitative RT-PCR assay of relative TOX3 mRNA expression in 22 pairs of human clinical ccRCC tissues (T) and adjacent noncancerous tissues (N, left panel), and paired Student *t*-test result with relative expression to internal reference *ACTB* showed in the right panel ($p < 0.001$). (B) Western blot assay of TOX3 protein level in 8 pairs of human clinical ccRCC samples. (C) Representative IHC staining of TOX3 in primary T1-T4 stage and primary metastatic (PM-T) ccRCC tissues compared with paired adjacent noncancerous tissues. (D–E) TOX3 staining scores in clinical T1-T4 stage tumors (D) and TNM stage tumors (E). (F) Frequency of TOX3 staining scores in noncancerous tissues (N), primary tumors without metastasis (P–T) and primary metastatic tumors (PM-T); Blue: 9–12, pink: 5–8, red: 0–4. (G) Western blot analysis of TOX3 protein level in RCC cell lines and control cell lines 293T and HK-2. (For interpretation of the references to color in this figure legend, the reader is referred to the Web version of this article.)

deficiency (Fig. 1F–G), with no prognostic difference observed in pRCC patients (Supplementary Fig. S2D). These data suggest that loss of TOX3 may play an important role in the development of ccRCC.

3.2. Validation of TOX3 down-regulation in ccRCC clinical specimens and cell lines

After the identification of TOX3, we detected TOX3 with its family genes TOX2 and TOX4 in 22 pairs of ccRCC tissues and adjacent non-cancerous tissues by qRT-PCR: as compared with adjacent non-cancerous tissues, 19 of 22 (86.4%) cancerous specimens showed decreased TOX3 mRNA level ($p < 0.001$, Fig. 2A), with no significant differences in levels of TOX2 and TOX4 (Supplementary Figs. S3A–B). Consistently, the reduced expression of TOX3 was further confirmed at the protein level by western blot analysis (Fig. 2B) in 8 paired surgical resected specimens and by IHC assay (Fig. 2C). Furthermore, expression of TOX3 decreased gradually with increased clinical T stage of ccRCC tissues (Fig. 2C–D). Moreover, advanced TNM stage was associated with low TOX3 staining score (Fig. 2E). To further investigate the association between TOX3 protein level and ccRCC metastasis, clinical specimens were divided into three groups — N (adjacent noncancerous tissues), P-T (primary tumors without metastasis) and PM-T (primary metastatic tumors) — to assess the staining intensity of TOX3. PM-T specimens showed high frequency of low TOX3 staining scores compared with the two other groups (Fig. 2F, Supplementary Fig. S3C).

To determine the clinical relevance of TOX3 expression in human ccRCC, we used IHC of TOX3 in 151 ccRCC patient specimens. TOX3 expression was not correlated with gender and age, with no significant correlation between TOX3 level and N stage or recurrence ($p > 0.05$, Table 1). However, TOX3 staining score was low in tumors with high histological grade (3 + 4) ($p < 0.050$) or advanced T stage (T3 + T4) ($p < 0.001$) (Table 1). Representative images of microvascular invasion were showed in Supplementary Figs. S3D–E, accompanying vein next to artery was filled with the tumor thrombus, CD31 staining was performed to further confirm the microvascular sites. Tumors with low TOX3 expression frequently showed distant metastasis ($p = 0.035$) and microvascular invasion ($p = 0.003$) (Table 1).

In addition, we further detected the expression of TOX3 in the human embryonic kidney cell line 293T, the immortal renal tubular epithelial cell line HK-2 and a panel of RCC cell lines. As compared with

Table 1
Correlation of TOX3 expression to clinicopathological features in 151 ccRCC patients.

Variables		TOX3		*p*-value
		Low	High	
Gender	male	58 (61.7%)	34 (59.6%)	0.802
	female	36 (38.3%)	23 (40.4%)	
Age, y	≤50	28 (29.8%)	16 (28.1%)	0.822
	> 50	66 (70.2%)	41 (71.9%)	
Histological grade	1	14 (14.9%)	14 (24.6%)	**0.050**
	2	41 (43.6%)	30 (52.6%)	
	3 + 4	39 (41.5%)	13 (22.8%)	
T stage	T1	42 (44.7%)	43 (75.4%)	**< 0.001**
	T2	17 (18.1%)	10 (17.5%)	
	T3+T4	35 (37.2%)	4 (7.0%)	
N stage	N0	88 (93.6%)	54 (94.7%)	1.000
	N1	6 (6.4%)	3 (5.3%)	
Distant metastasis	M0	75 (79.8%)	53 (93.0%)	**0.035**
	M1	19 (20.2%)	4 (7.0%)	
Recurrence	no	86 (91.5%)	56 (98.2%)	0.154
	yes	8 (8.5%)	1 (1.8%)	
Microvascular invasion	no	69 (73.4%)	53 (93.0%)	**0.003**
	yes	25 (26.6%)	4 (7.0%)	

Note: TNM stage grouping was assigned according to the 2009 TNM staging classification system. Statistical significance was calculated by the Fisher exact test or the Chi-square test.

293T and HK-2 cells, RCC cells showed lower TOX3 expression (Fig. 2G). ACHN and Caki-1 cells were derived from metastatic sites of pleural effusion and skin, respectively, and 786-O cells were originally derived from a primary tumor of an individual with extensive metastatic disease [30]. These three cell lines showed lower TOX3 protein level than two other cell lines, 769-P and A498.

3.3. Loss of TOX3 promotes ccRCC aggressiveness in vitro

To uncover the role of TOX3 deficiency in ccRCC progression, we overexpressed TOX3 in the ccRCC cell lines 786-O and 769-P and knocked down TOX3 in 769-P cells. MTT assay revealed remarkably enhanced growth in 769-P cells that were transiently transfected with TOX3 siRNAs as compared with the siRNA normal control (siNC) group (Fig. 3A). Conversely, TOX3 overexpression in 786-O and 769-P cells significantly inhibited cell proliferation as compared with the empty vector group.

Afterwards, the lentivirus system was used to construct stable TOX3 overexpression and knockdown cell lines (Fig. 3B, Supplementary Figs. S4A–C). Double-color immunofluorescent staining showed that overexpressed TOX3 protein was mainly localized in the nuclei of most 786-O and 769-P cells (Fig. 3C, Supplementary Fig. S4E).

Transwell and wound-healing assays were used to assess migratory and invasive activity of ccRCC cells. Cell migration and invasion was accelerated when TOX3 was stably knocked down in 769-P cells (Fig. 3F). Correspondingly, stable overexpression of TOX3 notably reduced 786-O and 769-P cells migration and invasion (Fig. 3D–E). Two molecular phenotype markers related to the EMT process, E-cadherin and fibronectin, were detected by immunofluorescent staining. E-cadherin was significantly upregulated with TOX3 overexpression and decreased with TOX3 knockdown, and fibronectin showed the opposite pattern (Fig. 3G). All these results, imply that TOX3 might suppress the EMT of ccRCC cells and therefore inhibit metastasis.

3.4. TOX3 inhibits EMT by transcriptionally repressing SNAI1 and SNAI2

To reveal the potential mechanism of TOX3 inhibiting ccRCC aggressiveness, we analyzed the gene sets altered by TOX3 expression by using GSEA in TCGA ccRCC database. EMT was the second top pathway negatively associated with TOX3 augmentation (NES = -4.00, $p < 0.001$, Fig. 4A–B, supplementary file 2) which indicated that TOX3 was likely to inhibit the EMT.

Then, we used qRT-PCR to analyze a series of classical molecular markers and EMT-related transcription factors, including CDH1, CDH2, VIM, FN1, FOXC2, ZEB1, SNAI1 and SNAI2. In 786-O and 769-P cells with stable TOX3 overexpression, CDH1 mRNA level was significantly increased, whereas that of the mesenchymal marker FN1and EMT-inducing transcription factors SNAI1 and SNAI2 was inhibited (Fig. 4C). Also, when we knocked down TOX3 769-P cells, the mRNA levels of FN1, SNAI1 and SNAI2 were increased and that of CDH1 was decreased (Fig. 4C). Similar results were found on western blot assay (Fig. 4D). The malignant shift of marker expression was also reflected in cellular morphological changes: overexpression of TOX3 in 786-O and 769-P cells disturbed cell polarity, whereas TOX3 knockdown in 769-P cells transformed cells from a rounded, epithelial type morphology to a spindle-shaped, mesenchymal-like contour (Fig. 4E).

Loss of E-cadherin is considered as the feature of activated EMT and is directly driven by SNAI1. Recent studies also discovered that Slug could modulate E-cadherin expression [22,24]. TOX3 may inhibiting SNAI1 and SNAI2 expression and lead to deregulation of E-cadherin. The inverse correlation between TOX3 and SNAI1 or SNAI2 was further confirmed in clinical ccRCC tissues. SNAI1 or SNAI2 expression was progressively reduced with TOX3 overexpression (SNAI1: R [2] = 0.725, $p = 0.0036$; SNAI2: R [2] = 0.482, $p = 0.038$) (Fig. 4F).

Previous study showed that TOX3 could bind to BRCA1 promoter and downregulate BRCA1 promoter activity in breast cancer [31]. Similarly, we investigated whether TOX3 binds to the promoter of SNAI1 and SNAI2 by ChIP assay. Results showed that TOX3 binds to the target segments more than does IgG (Fig. 4G), which indicates that TOX3 could transcriptionally suppress SNAI1 and SNAI2 expression. Then we use Transwell assay to identify the combined biologic effect of TOX3 and SNAI1 or SNAI2. The suppressed migration and invasion of 786-O cells due to TOX3 overexpression was restored with transient transfection of SNAI1 or SNAI2 (Fig. 4H). Thus, TOX3 might inhibit EMT via binding to promoters of SNAI1 and SNAI2 and suppressing their transcription.

3.5. Tox3 overexpression suppresses cancer cell growth and metastasis in vivo

We further investigated the comprehensive function of TOX3 in mice. We overexpressed Tox3 in the murine RCC cell line Renca (Fig. 5A, Supplementary Fig. S4D). Cells of different groups were subcutaneously injected into the right side of mice. At 2 weeks later, stable overexpression of Tox3 significantly reduced the volume ($p < 0.05$) and weight ($p < 0.01$) of subcutaneous tumors compared with the control group (Fig. 5B–C).

The progression of lung metastasis was evaluated 4 weeks after Renca cells were injected into the tail vein of mice. Representative gross views of lung samples and hematoxylin and eosin-stained slides of lungs dissected from each group are shown in Fig. 5D and E. The size of metastatic nodules was smaller in Tox3-overexpressed mice and the number of pulmonary metastatic nodules was significantly lower ($p < 0.01$, Fig. 5F). Moreover, we detected the expression of Tox3, Snail1 and Slug in pulmonary metastatic lesions. As compared with controls, Tox3-overexpressed mice showed significant Tox3 upregulation and down regulation of Snail1 and Slug (Fig. 5G). Accordingly, Tox3 overexpression prolonged the survival of mice (Fig. 5H).

Prognostic values with the combination of TOX3 level and SNAI1 or SNAI2 levels were evaluated to obtain the guidance in predicting patient outcome with these gene patterns. We analyzed the clinical data for ccRCC patients in the TCGA database. Patients with low TOX3 and high SNAI1 levels exhibited the worst clinical outcome (Fig. 5I, left). In agreement, patients with high TOX3 and low SNAI1 levels had the longest OS ($p < 0.0001$). Similarly, patients with low TOX3 and high SNAI2 levels had the shortest OS ($p < 0.0001$, Fig. 5I, right).

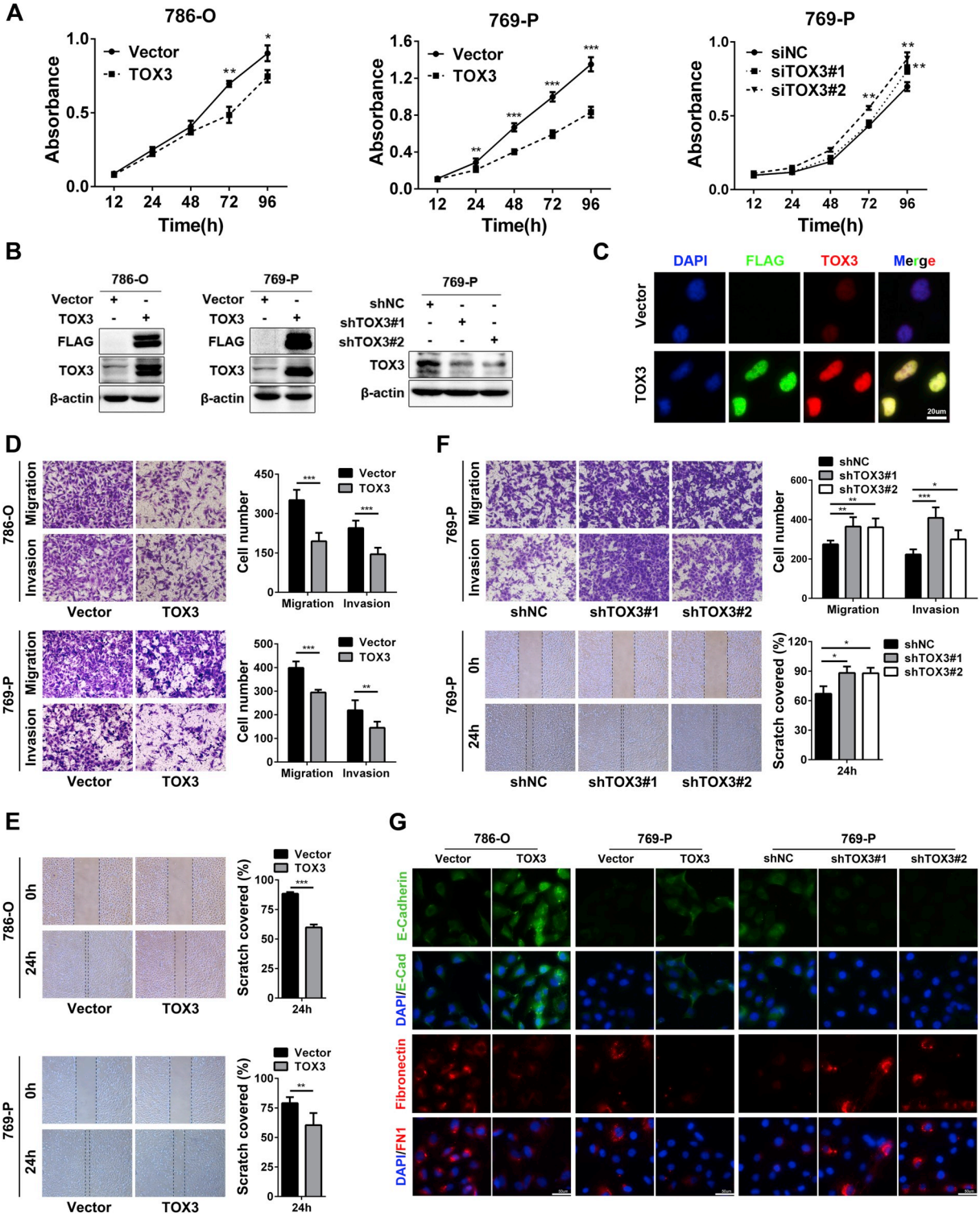

Fig. 3. Loss of TOX3 promotes ccRCC aggressiveness *in vitro*. (A) MTT assay of TOX3 overexpression in 786-O and 769-P cells suppressing proliferation velocity, whereas knockdown of TOX3 promoted tumor growth in 769-P cells. (B) Efficiency of overexpression and knockdown of TOX3 validated in related cell lines using western blot. (C) Representative immunofluorescence images of the location of TOX3 overexpression in 786-O cells. Scale bar = 20 μm. (D–F) TOX3 augmentation significantly reduced migration and invasion of 786-O and 769-P cells on Transwell assay (D), and migration on wound-healing assay (E). TOX3 knockdown promoted tumor aggressiveness in 769-P cells (F). (G) Immunofluorescent staining to detect altered EMT-related proteins (E-cadherin and fibronectin) after TOX3 overexpression or downregulation in related cell lines. Scale bar = 50μm. *, $p < 0.05$, **, $p < 0.01$, ***, $p < 0.001$.

3.6. Aberrant CpG methylation of promoter reduced TOX3 expression

Aberrant promoter hypermethylation is one of the causes of tumor suppressor silencing in RCC [32–35]. To determine whether DNA methylation is associated with TOX3 downregulation in ccRCC tissues, we analyzed DNA methylation microarray data in the TCGA database. Ten CpG probes located at the promoter region of TOX3 were identified (Supplementary Fig. S5A); Methylation levels of the TOX3 promoter

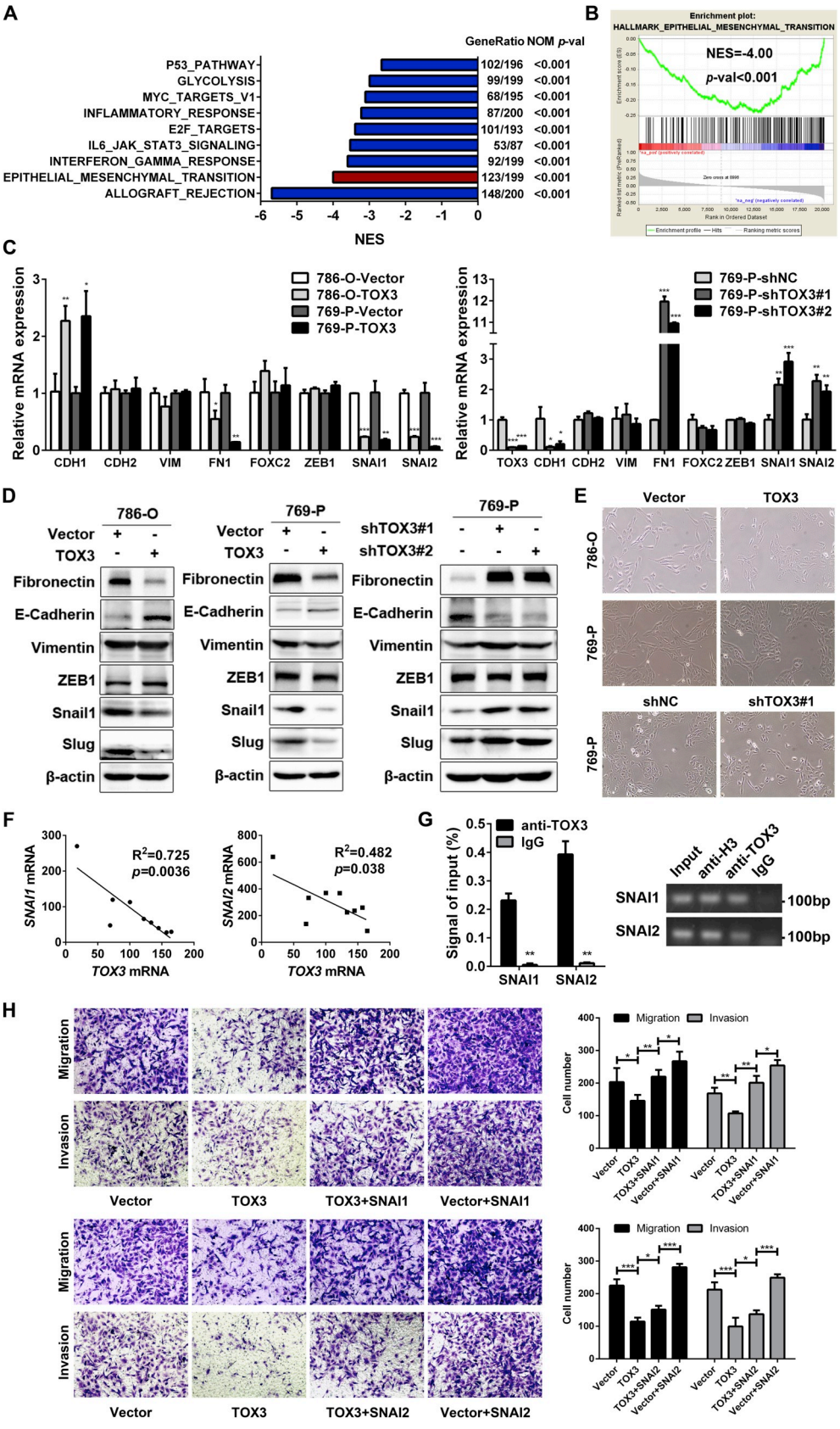

Fig. 4. TOX3 inhibits EMT by transcriptionally repressing SNAI1 and SNAI2. (A) Top differentially expressed cancer-related gene sets with low TOX3 expression in the TCGA ccRCC cohort. (B) GSEA output of altered genes in the EMT pathway by TOX3 high and low expression groups from the TCGA ccRCC cohort [normalized enrichment score (NES) = −4.00, $p < 0.001$]. (C) Relative mRNA expression (D) protein expression of EMT-related cellular markers and transcription factors in cell lines. (E) Representative images of morphologic alteration of cells with the TOX3 overexpression or knockdown. (F) Correlation analysis of mRNA levels of TOX3 and SNAI1 or SNAI2 in ccRCC samples from GSE781. (G) ChIP-qPCR assay of TOX3, normal rabbit IgG and positive control Histone 3. (H) Effect of restored expression of SNAI1 or SNAI2 on migration and invasion of TOX3-overexpressed 786-O cells. *, $p < 0.05$, **, $p < 0.01$, ***, $p < 0.001$.

and four of 10 CpG probes (cg02709321, cg26648818, cg01404163, cg027934521) were significantly increased in ccRCC tissues, and were further increased in primary metastatic ccRCC tissues (Fig. 6C). Accordingly, the hypermethylation of TOX3 promoter and the four CpG probes was negatively correlated with TOX3 expression ($p < 0.0001$, Fig. 6A–B), whereas the methylation of the remaining six CpG probes was not significantly correlated with TOX3 expression or metastatic status (Supplementary Figs. S5B–C).

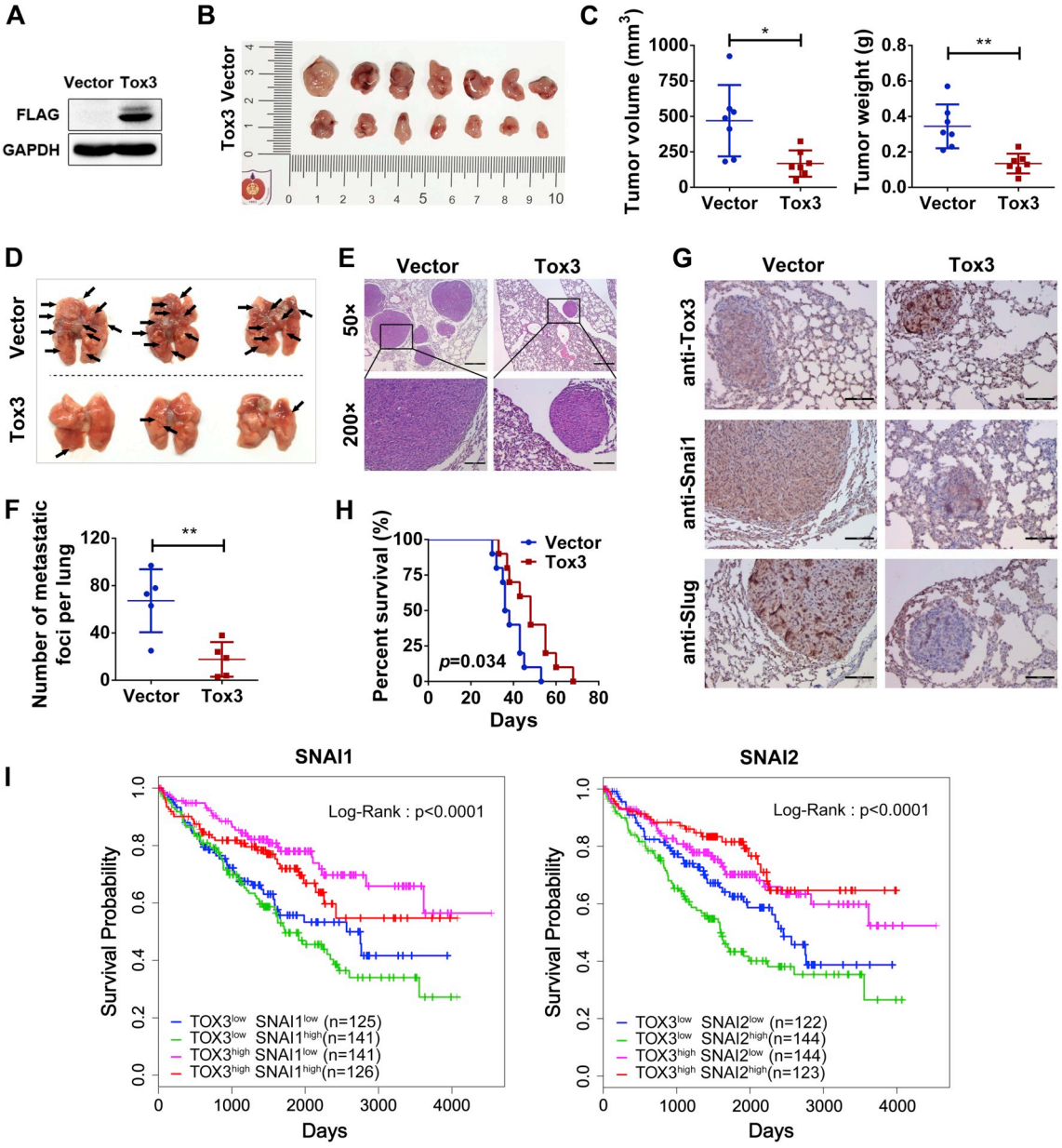

Fig. 5. Tox3 overexpression suppresses growth and metastasis of renal cancer cells in mice. (A) Efficiency of Tox3 overexpression validated in Renca cells. (B) Dissected tumors from subcutaneously injected mice with Tox3-overexpression or control cells; n = 7/group. (C) Tumor volume and weight of subcutaneous tumors. (D) Representative gross view of lung samples with metastatic nodules (black arrows, metastatic nodules). (E) Hematoxylin and eosin-stained slides of lungs. Scale bar of upper panel = 400 μm. (F) Number of the pulmonary metastatic lesions; n = 5/group. (G) Immunohistochemistry of Tox3, snail1 and slug in dissected lung samples. Scale bar = 100 μm. (H) Overall survival of mice with cells injected in tail veins; n = 10/group. (I) Kaplan-Meier analysis of overall survival of ccRCC patients in the TCGA database by mRNA level of TOX3 and SNAI1 or SNAI2. Cut-off values of Log_2(normalized count) for TOX3, SNAI1 and SNAI2 were 5.88, 7.33 and 7.817, respectively. *P* values were calculated by log-rank test. *, $p < 0.05$, **, $p < 0.01$.

Renal cancer cells with relatively low TOX3 expression were treated with concentrations of the DNA methyltransferase inhibitor 5-Aza, which led to a dose-dependent restoration of TOX3 expression, which suggests a negative correlation between DNA methylation and TOX3 expression (Fig. 6D–E). Taken together, these data indicate that functional loss of TOX3 in ccRCC is attributed to hypermethylation of four potential CpG probes located in the TOX3 promoter region.

After that, we further evaluated the therapeutic effect of 5-Aza *in vivo*. After treatment of 5-Aza, mice showed significant lower luminescent signal in lungs (Fig. 6F–G), HE staining of pulmonary slides also showed less and smaller lung metastatic nodules in treatment group (Fig. 6H). Tox3 expression was restored after 5-Aza treatment (Fig. 6I). Beyond that, mice also showed lower subcutaneous tumor burden (Supplementary Figs. 6A–C).

4. Discussion

In this study, we demonstrated that TOX3 participates in suppressing RCC progression. TOX3 was downregulated in ccRCC tissues from GEO datasets and the TCGA database as well as in clinical cancer specimens from our department as compared with normal tissues. Loss of TOX3 was correlated with advanced T stage, distant metastasis, cancer recurrence and microvascular invasion and showed strong prognostic value for OS and MFS in ccRCC patients. Microvascular invasion was tightly correlated with adverse clinicopathological features and was an independent predictor of metastatic spread in RCC; it occurs in nearly 1

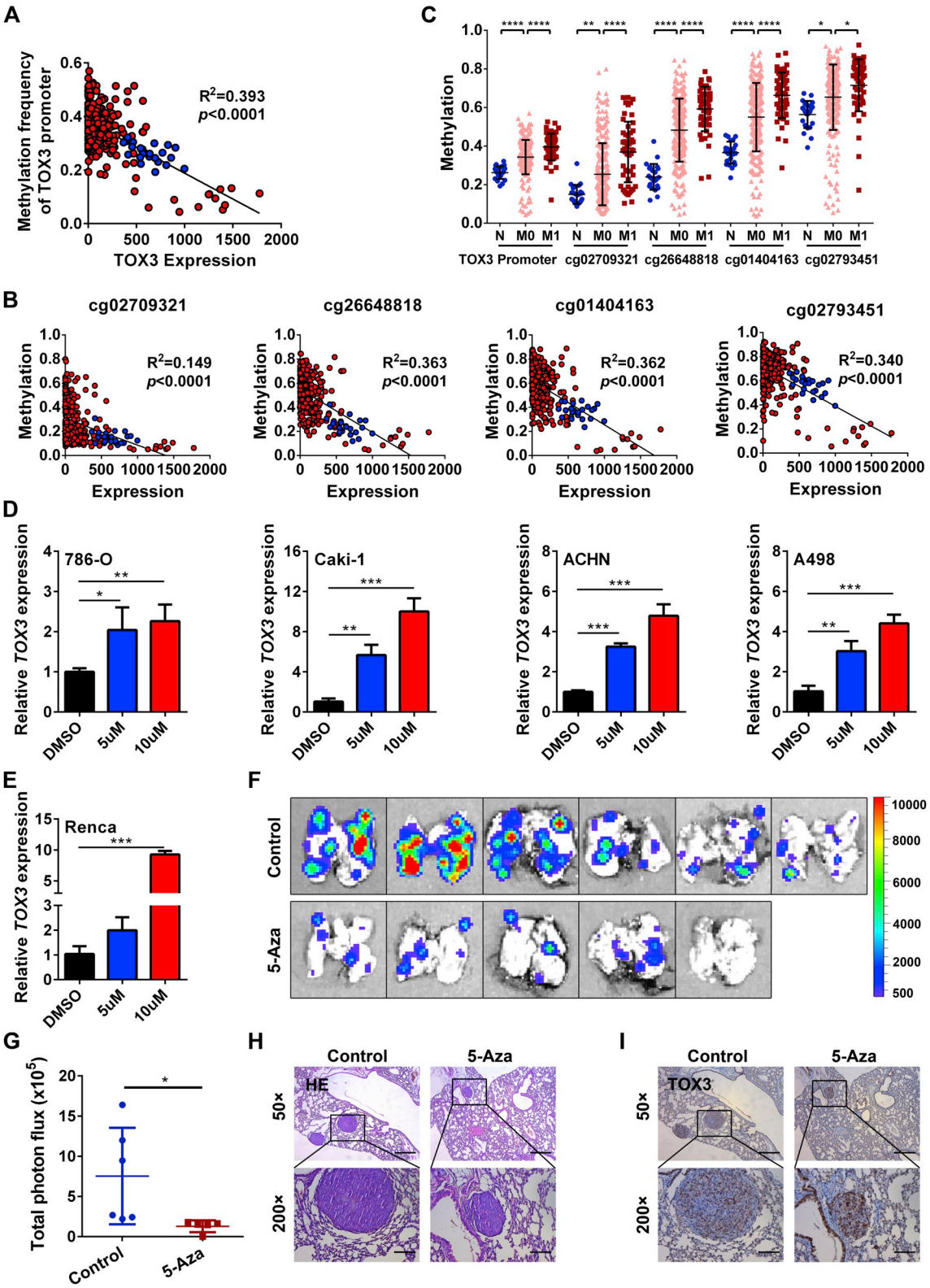

Fig. 6. Aberrant CpG methylation associated with downregulation of TOX3. (A) Correlation of methylated level of promoter region and TOX3 mRNA level in the TCGA ccRCC cohort (R [2] = 0.393, $p < 0.0001$). Blue spot, normal kidney tissues; red spot, ccRCC tissues. (B) Correlation of TOX3 mRNA level and methylation level of four CpG probes (cg02709321, cg26648818, cg01404163, cg027934521) ($p < 0.0001$). (C) Methylation levels of TOX3 promoter and four specific CpG probes in M0 ccRCC tissues, and primary M1 ccRCC tissues. M0: without metastasis; M1: with metastasis. (D–E) Expression changes of TOX3 mRNA in RCC cells treated with concentrations of 5-azacytidine versus DMSO. (F–G) Bioluminescent images of resected lungs after 5-Aza treatment. (H) Hematoxylin and eosin staining of section from the lung specimen. (I) IHC staining showed the TOX3 level change in tumor cells after 5-Aza treatment. *, $p < 0.05$, **, $p < 0.01$, ***, $p < 0.001$. (For interpretation of the references to color in this figure legend, the reader is referred to the Web version of this article.)

of 5 RCC patients [24], which involved 29/151 (19.2%) patients in this study. The significant correlation between TOX3 level and microvascular invasion indicates that TOX3 may promote RCC metastasis via facilitating cancer cells cross the vessel wall to form tumor thrombus, then spread to distant organs.

Several studies found that the SNPs of TOX3 may be associated with risk of breast and lung cancer [12,13], but little research has focused on the function of TOX3 in altering cancer aggressiveness. Research by Chouchane et al. found that TOX3 may bind to the CREB and BRCA1 promoter and downregulate BRCA1 promoter activity, and deficiency of TOX3 could suppress the proliferation of the breast cancer cell line [12]. However, another study by Moore et al. had the opposite result: silencing TOX3 could promote the growth of breast cancer cell lines [31]. Therefore, the ability of TOX3 to alter the biology of cancer cells needs to be further clarified. In this study, restoring the expression of TOX3 suppressed the proliferation, migration and invasion of RCC cells. In contrast, TOX3 knockdown could promote the aggressiveness of 769-P cells *in vitro*. These results confirmed the role of TOX3 in suppressing tumor aggressiveness in RCC cell lines.

To determine the downstream signaling pathways, GSEA was used to identify the probable pathway related to TOX3. The EMT process was significantly promoted with TOX3 deficiency. In this study, a series of phenotype markers and EMT-related transcriptional factors were detected. E-cadherin was downregulated and fibronectin, snai1 and slug were upregulated when TOX3 expression was suppressed. Moreover, the expression of SNAI1 and SNAI2 was negatively associated with TOX3 level in the GSE781 dataset. Results of ChIP assay confirmed the direct binding of TOX3 protein and the SNAI1 or SNAI2 promoter region. Hence, the inhibition of EMT is due to TOX3 binding to the promoter region of key transcriptional factors of the EMT pathway, SNAI1 and SNAI2, then suppressing their expression. Furthermore, TOX3 was associated with *P53* and *MYC* pathways (Fig. 4A), so TOX3 may be involved in modulating these pathways as well to suppress ccRCC aggressiveness, which needs further research.

Bone-marrow-derived cells, including macrophages, neutrophils and myeloid-derived suppressor cells, were found involved in the formation of metastatic lesions [36–39]. Meanwhile, the structure and function of TOX3 protein are highly conserved among species, so BALB/c mice were selected as experimental animals for *in vivo* experiments. Overexpression of Tox3 inhibited tumor growth and metastasis and prolonged the life of mice. In Fig. 5I, TOX3 high and SNAI2 high seemed to show better OS than TOX3 high and SNAI2 low subgroup, but in fact the *p*-value of these two curves pairwise comparison is 0.32 and not statistic significant. As for the unexpected trend of this curve, one possible explanation is SNAI gene family were also regulated by other pathways, e.g. WNT and TGFβ signaling pathways (*17*). Here we calculated the relationship between RNA levels and prognosis, another possible explanation is the lack of correlation between the RNA levels and the activities of proteins and indicate the probable presence of post-translational control.

Epigenetic regulation of TOX subfamily genes have been evaluated in lung cancer and breast cancer in previous studies. Dense methylation of TOX3 promoter was detected in some lung and breast tumors, with unmethylated in all normal samples [40]. In addition, Han et al. also found that methylation level of four CpG probes (cg02709321, cg11410436, cg26648818, and cg01404163) in the promoter region were also associated with TOX3 expression in breast tumors [41], which was expanded to ten CpG probes in our work. Correspondingly, three CpG probes (cg02709321, cg26648818, and cg01404163) were also associate with functional loss of TOX3 in ccRCC, furthermore, same pattern was discovered in cg02793451 probe. Taken together, hypermethylation of TOX3 promoter was common in various cancer types and may involve in several specific CpG sites.

In conclusion, we elucidated that the TOX3-mediated transcriptional suppression of SNAI1 and SNAI2 represses the migration and invasion potential of ccRCC cells, which plays an important role in the malignant progression of human ccRCC and has therapeutic implications.

Disclosure of potential conflicts of interest

The authors declare no potential conflicts of interest exist.

Acknowledgments

This work was supported by grants from the National Natural Science Foundation of China (81502203, 81772710, 81802535), the National Natural Science Foundation of Jiangsu Province (BK20150097), the Project of Invigorating Health Care through Science, Technology and Education Jiangsu Provincial Key Medical Discipline (ZDXKB2016014), the “Summit of the Six Top Talents” Program of Jiangsu Province (SWYY-084), Postdoctoral Scientific Research Project of China (2017M621729) and the Postdoctoral Research Foundation of Jiangsu Province (1701021B), Nanjing Medical Science and technique Development Foundation (QRX17139).

Appendix A. Supplementary data

Supplementary data to this article can be found online at https://doi.org/10.1016/j.canlet.2019.02.020.

References

[1] R.L. Siegel, K.D. Miller, A. Jemal, Cancer statistics, 2016, Ca - Cancer J. Clin. 66 (2016) 7–30.
[2] Genetics of kidney cancer (renal cell cancer) (PDQ(R)): health Professional Version, PDQ Cancer Information Summaries, National Cancer Institute, Bethesda, MD, 2002.
[3] R.J. Motzer, et al., Overall survival and updated results for sunitinib compared with interferon alfa in patients with metastatic renal cell carcinoma, J. Clin. Oncol. 27 (2009) 3584–3590.
[4] C.N. Sternberg, et al., Pazopanib in locally advanced or metastatic renal cell carcinoma: results of a randomized phase III trial, J. Clin. Oncol. 28 (2010) 1061–1068.
[5] J.M. Randall, F. Millard, R. Kurzrock, Molecular aberrations, targeted therapy, and renal cell carcinoma: current state-of-the-art, Cancer Metastasis Rev. 33 (2014) 1109–1124.
[6] E. O'Flaherty, J. Kaye, TOX defines a conserved subfamily of HMG-box proteins, BMC Genomics 4 (2003) 13.
[7] M.R. Christopher, P.D. Cary, C. Crane-Robinson, P.C. Driscoll, D.G. Norman, Solution structure of a DNA-binding domain from HMG1, Nucleic Acids Res. 21 (1993) 3427–3436.
[8] C.A. Bewley, A.M. Gronenborn, G.M. Clore, MINOR GROOVE-BINDING ARCHITECTURAL PROTEINS: structure, function, and DNA recognition, Annu. Rev. Biophys. Biomol. Struct. (1998) 105–131.
[9] S.H. Yuan, Z. Qiu, A. Ghosh, TOX3 regulates calcium-dependent transcription in neurons, Proc. Natl. Acad. Sci. U. S. A. 106 (2009) 2909–2914.
[10] S. Dittmer, et al., TOX3 is a neuronal survival factor that induces transcription depending on the presence of CITED1 or phosphorylated CREB in the transcriptionally active complex, J. Cell Sci. (2011) 252–260.
[11] D. Bastien, et al., IL-1alpha gene deletion protects oligodendrocytes after spinal cord injury through upregulation of the survival factor Tox3, J. Neurosci. 35 (2015) 10715–10730.
[12] R. Cowper-Sal lari, et al., Breast cancer risk-associated SNPs modulate the affinity of chromatin for FOXA1 and alter gene expression, Nat. Genet. 44 (2012) 1191–1198.
[13] C. Jiang, et al., The breast cancer susceptibility-related polymorphisms at the TOX3/LOC643714 locus associated with lung cancer risk in a Han Chinese population, Oncotarget 7 (2016).
[14] B. De Craene, G. Berx, Regulatory networks defining EMT during cancer initiation and progression, Nat. Rev. Canc. 13 (2013) 97–110.
[15] T. Brabletz, To differentiate or not — routes towards metastasis, Nat. Rev. Canc. 12 (2012) 425–436.
[16] M.A. Nieto, The ins and outs of the epithelial to mesenchymal transition in health and disease, Annu. Rev. Cell Dev. Biol. 27 (2011) 347–376.
[17] S. Lamouille, J. Xu, R. Derynck, Molecular mechanisms of epithelial-mesenchymal transition, Nat. Rev. Mol. Cell Biol. 15 (2014) 178–196.
[18] C.G. Wood, J.A. Copland, Loss of E-cadherin expression is associated with metastatic progression in human renal cell carcinoma, J. Urol. 169 (2003) 145–146.
[19] D. Ni, et al., Downregulation of FOXO3a promotes tumor metastasis and is associated with metastasis-free survival of patients with clear cell renal cell carcinoma, Clin. Cancer Res. 20 (2014) 1779–1790.
[20] L.M. Knowles, et al., Integrin alphavbeta3 and fibronectin upregulate Slug in cancer cells to promote clot invasion and metastasis, Cancer Res. 73 (2013) 6175–6184.

[21] T. Ni, et al., Snail1-dependent p53 repression regulates expansion and activity of tumour-initiating cells in breast cancer, Nat. Cell Biol. 18 (2016) 1221–1232.
[22] J. Ju, et al., NatD promotes lung cancer progression by preventing histone H4 serine phosphorylation to activate Slug expression, Nat. Commun. 8 (2017) 928.
[23] A.S. Sharili, S. Allen, K. Smith, J. Price, I.M. McGonnell, Snail2 promotes osteosarcoma cell motility through remodelling of the actin cytoskeleton and regulates tumor development, Cancer Lett. 333 (2013) 170–179.
[24] N. Kroeger, et al., Prognostic value of microvascular invasion in predicting the cancer specific survival and risk of metastatic disease in renal cell carcinoma: a multicenter investigation, J. Urol. 187 (2012) 418–423.
[25] R. Beroukhim, et al., Patterns of gene expression and copy-number alterations in von-hippel lindau disease-associated and sporadic clear cell carcinoma of the kidney, Cancer Res. 69 (2009) 4674–4681.
[26] J. Jones, et al., Gene signatures of progression and metastasis in renal cell cancer, Clin. Cancer Res. 11 (2005) 5730–5739.
[27] M.V. Yusenko, et al., High-resolution DNA copy number and gene expression analyses distinguish chromophobe renal cell carcinomas and renal oncocytomas, BMC Canc. 9 (2009) 152.
[28] M.L. Gumz, et al., Secreted frizzled-related protein 1 loss contributes to tumor phenotype of clear cell renal cell carcinoma, Clin. Cancer Res. 13 (2007) 4740–4749.
[29] M.E. Lenburg, L.S. Liou, Previously Unidentified Changes in Renal Cell Carcinoma Gene Expression Identified by Parametric Analysis of Microarray Data, BMC Cancer, 2003.
[30] R.D. Williams, A.Y. Elliott, N. Stein, E.E. Fraley, In vitro cultivation of human renal cell cancer. II. Characterization of cell lines, In Vitro 14 (1978) 779–786.
[31] J. Shan, et al., TNRC9 downregulates BRCA1 expression and promotes breast cancer aggressiveness, Cancer Res. 73 (2013) 2840–2849.
[32] R.E. Banks, et al., Genetic and epigenetic analysis of von Hippel-Lindau (VHL) gene alterations and relationship with clinical variables in sporadic renal cancer, Cancer Res. 66 (2006) 2000–2011.
[33] M.R. Morris, F. Latif, The epigenetic landscape of renal cancer, Nat. Rev. Nephrol. 13 (2016) 47–60.
[34] N. Cancer, Genome Atlas Research, Comprehensive molecular characterization of clear cell renal cell carcinoma, Nature 499 (2013) 43–49.
[35] W.J. Kim, Z. Gersey, Y. Daaka, Rap1GAP regulates renal cell carcinoma invasion, Cancer Lett. 320 (2012) 65–71.
[36] J. Kim, J.S. Bae, Tumor-Associated Macrophages and Neutrophils in Tumor Microenvironment, Mediat Inflamm, 2016.
[37] Y. Liu, et al., Tumor exosomal RNAs promote lung pre-metastatic niche formation by activating alveolar epithelial TLR3 to recruit neutrophils, Cancer Cell 30 (2016) 243–256.
[38] M. Ouzounova, et al., Monocytic and granulocytic myeloid derived suppressor cells differentially regulate spatiotemporal tumour plasticity during metastatic cascade, Nat. Commun. 8 (2017) 14979.
[39] L. Yang, et al., Abrogation of TGF beta signaling in mammary carcinomas recruits Gr-1 + CD11b + myeloid cells that promote metastasis, Cancer Cell 13 (2008) 23–35.
[40] M. Tessema, et al., Differential epigenetic regulation of TOX subfamily high mobility group box genes in lung and breast cancers, PLoS One 7 (2012) e34850.
[41] Y.J. Han, J. Zhang, Y. Zheng, D. Huo, O.I. Olopade, Genetic and epigenetic regulation of TOX3 expression in breast cancer, PLoS One 11 (2016) e0165559.